



Título artículo / Títol article: Harnessing Infrared Photons for Photoelectrochemical Hydrogen Generation. A PbS Quantum Dot Based “Quasi-Artificial Leaf”

Autores / Autors: Trevisan, Roberto ; Rodenas, Pau ; González Pedro, Victoria ; Sima, Cornelia ; Sánchez, Rafael ; Barea Berzosa, Eva María ; Mora Seró, Iván ; Fabregat Santiago, Francisco ; Giménez Juliá, Sixto

Revista: The Journal of Physical Chemistry Letters (2013), vol. 4, no 1

Versión / Versió: Postprint

Cita bibliográfica / Cita bibliogràfica (ISO 690): TREVISAN, Roberto, et al. Harnessing Infrared Photons for Photoelectrochemical Hydrogen Generation. A PbS Quantum Dot Based “Quasi-Artificial Leaf”. The Journal of Physical Chemistry Letters, 2013, vol. 4, no 1, p. 141-146.

url Repositori UJI: <http://hdl.handle.net/10234/89433>

# Harnessing Infrared Photons for Photoelectrochemical Hydrogen Generation. A PbS Quantum Dot Based “Quasi-Artificial Leaf”

Roberto Trevisán,<sup>1</sup> Pau Ródenas,<sup>1</sup> Victoria González-Pedro,<sup>1</sup> Cornelia Sima,<sup>1,2,3</sup> Rafael Sánchez,<sup>1</sup> Eva M. Barea,<sup>1</sup> Iván Mora-Seró,<sup>1,\*</sup> Francisco Fabregat-Santiago,<sup>1</sup> Sixto Giménez<sup>1,\*</sup>

<sup>1</sup> Photovoltaics and Optoelectronic Devices Group, Departament de Física, Universitat Jaume I, 12071 Castelló, Spain

<sup>2</sup> National Institute of Lasers, Plasma and Radiation Physics, Atomistilor 409 street, P.O. Box MG 36 Bucharest-Magurele, 077125, Romania

<sup>3</sup> University of Bucharest, Faculty of Physics, Atomistilor 405 street, MG-11 Bucharest-Magurele, 077125, Romania

\*Email: [sero@uji.es](mailto:sero@uji.es), [sjulia@fca.uji.es](mailto:sjulia@fca.uji.es)

## Abstract

Unassisted hydrogen generation by using quantum dot based heterostructures has emerged as a promising strategy to develop artificial photosynthesis devices. In the present study, we sensitize mesoporous TiO<sub>2</sub> electrodes with *in-situ* deposited PbS/CdS quantum dots (QDs), aiming at harvesting light in the visible and the near infrared for hydrogen generation. This heterostructure exhibits a remarkable photocurrent of 6 mA·cm<sup>-2</sup> leading to 60 ml·cm<sup>-2</sup>·day<sup>-1</sup> hydrogen generation in a three electrode photoelectrochemical cell. Confirmation of the contribution of infrared photons to H<sub>2</sub> generation was provided by the incident-photon-to-current-efficiency (IPCE) action spectrum, and the integrated current was in excellent agreement with that obtained through cyclic voltammetry. The main electronic processes (chemical capacitance, transport resistance and recombination resistance) were identified by impedance spectroscopy, which appears as a simple and reliable methodology to evaluate the limiting factors of these photoelectrodes. Based on this TiO<sub>2</sub>/PbS/CdS heterostructure, a “quasi-artificial leaf” has been developed, which has proven to produce hydrogen under simulated solar illumination at (4.30 ± 0.25) ml·cm<sup>-2</sup>·day<sup>-1</sup>

**Keywords:** Hydrogen generation, quantum dots, lead sulfide, cadmium sulfide, titanium dioxide, impedance spectroscopy

The provision of clean and renewable energy to satisfy the increasing human demands in the XXI century is one of the key challenges to sustain the present global social and economical model.<sup>1,2</sup> Sunlight offers a huge potentiality for global supply of renewable energy, provided that this energy can be stored for its use upon demand. In this context, photoelectrochemical hydrogen generation by water splitting with semiconductor materials constitutes the simplest conversion scheme, since H<sub>2</sub> can be produced with the only input of water and sunlight and H<sub>2</sub> combustion in hydrogen fuel cells leads to electricity with water as the only byproduct, resulting in a CO<sub>2</sub> neutral process.<sup>2-4</sup> The key challenge of this approach relies on whether this goal can be met in a cost-effective way on the terawatt scale.<sup>2</sup>

Since the seminal report of Fujishima and Honda in 1972 demonstrating the photocatalysis of TiO<sub>2</sub> for H<sub>2</sub> generation,<sup>5</sup> a dynamic search for the optimum semiconductor material and device configuration was launched, but crystallization of this research activity into a well developed technology has not been achieved yet, mainly because none of the explored materials simultaneously meet the different needed requirements for adequate device operation; i.e. a bandgap comprised between 1.9-2.2 eV, conduction and valence band edges straddling the water oxidation and hydrogen reduction potentials, good conductivity and low cost.<sup>2,4</sup> The novel developments in the fields of nanoscience and catalysis<sup>6</sup> have provided key elements and concepts to rationalize the search for promising materials and device architectures. Orthogonalization of light absorption and carrier diffusion,<sup>7-9</sup> quantum confinement,<sup>10</sup> band energetics engineering<sup>11</sup> and plasmonics<sup>12,13</sup> appear as fascinating strategies, which can be exploited to enhance the efficiencies of photoelectrochemical hydrogen generation devices. Sensitization of wide oxide semiconductors like ZnO or TiO<sub>2</sub> by chalcogenide quantum dots also provides a convenient heterostructured platform for photoelectrochemical H<sub>2</sub> generation. Indeed, this approach, has showed promising results: Hensel *et al.* showed the synergistic effect of N doping of TiO<sub>2</sub> nanowires and CdSe sensitization leading to photocurrents close to 3 mA·cm<sup>-2</sup>.<sup>14</sup> Combining ZnO nanowires with CdTe quantum dots, Chen *et al.* obtained photocurrents close to 2 mA·cm<sup>-2</sup> using a non-sacrificial hole scavenger.<sup>15</sup> Hierarchical ZnO/WO<sub>x</sub> nanowires cosensitized with CdSe/CdS led to promising photocurrents close to 12 mA·cm<sup>-2</sup> and light-to-chemical conversion efficiencies of 6%.<sup>16</sup> More recently, Luo *et al.* have highlighted the

importance of the controlled deposition of the light absorbing semiconductor (CdSe) on inverse opals of TiO<sub>2</sub>, achieving photocurrents of 15.7 mA·cm<sup>-2</sup> for hydrogen generation.

On the other hand, an optimal exploitation of the solar spectrum for photoelectrochemical energy conversion must entail the use of narrow bandgap semiconductors, like PbS, in order to harness infrared photons for photoelectrochemical conversion. Tada *et al.*<sup>17</sup> have reported a solar-to-hydrogen conversion efficiency of 1.15% and a hydrogen production rate of 5.2 ml·h<sup>-1</sup> employing a heterostructure based on mesoporous TiO<sub>2</sub> decorated with colloidal PbS quantum dots (under the application of bias). In the present study, we have developed a hybrid architecture based on a TiO<sub>2</sub> mesoporous frame functionalized with *in-situ* grown CdS/PbS QDs, targeting at an unassisted photoelectrochemical hydrogen generation device. The ultimate goal is achieving an artificial leaf converting visible and infrared photons into H<sub>2</sub>.

## Results and discussion

Colloidal PbS quantum dots have demonstrated to harness the infrared photons towards efficient solar hydrogen production.<sup>17</sup> We have incorporated *in-situ* grown PbS quantum dots onto a mesoporous TiO<sub>2</sub> structure together with CdS quantum dots to both enhance the visible response (see Supporting Information, Figure SI1) and stabilize the whole material.<sup>18</sup> The microscopic inspection of the material by SEM showed the mesoporous TiO<sub>2</sub> structure but did not reveal any morphological details of the PbS/CdS sensitizers (Supporting information, Figure SI2). The presence of PbS QDs was confirmed through XRD spectra carried out on TiO<sub>2</sub>/PbS structures (Supporting information, Figure SI3). High resolution TEM images (Supporting information, Figure SI4) reveal that both PbS and CdS appear as scattered nanoparticles (diameter below 10 nm) onto the mesoporous TiO<sub>2</sub> network, and covered by a ZnS layer.

The photoelectrochemical behavior of TiO<sub>2</sub>/PbS/CdS heterostructures in an aqueous solution containing 0.25 M Na<sub>2</sub>S and 0.35 M Na<sub>2</sub>SO<sub>3</sub> as sacrificial hole scavenger in the dark and under illumination is showed in Figure 1a. As a reference, results for TiO<sub>2</sub>/CdS are also included. It is clear that higher photocurrents are obtained when PbS is included in the heterostructures. At 0V vs RHE, a photocurrent of 2 mA·cm<sup>-2</sup> is obtained for both systems. Saturation of the photocurrent takes place at approximately 0.4 V vs RHE, with 6 mA·cm<sup>-2</sup> for TiO<sub>2</sub>/PbS/CdS and

3.5 mA·cm<sup>-2</sup> or TiO<sub>2</sub>/CdS. This equals 60 mL·cm<sup>-2</sup>·day<sup>-1</sup> and 35 mL·cm<sup>-2</sup>·day<sup>-1</sup> hydrogen generation rate, respectively, assuming a faradaic efficiency unity. The observed positive photocurrents correspond to hole injection from the heterostructured TiO<sub>2</sub>/QDs photoanode into the solution. The difference between the anodic and cathodic branches of the dark cyclic voltammetry curve, at potentials below 0V vs RHE (more visible for TiO<sub>2</sub>/CdS) is due to the chemical capacitance of TiO<sub>2</sub>, consistently with previous studies.<sup>19-21</sup>. Labeling experiments of the evolved gas at the Pt counterelectrode was collected in an inverted burette and analyzed. The results for TiO<sub>2</sub>/PbS/CdS are showed Figure 1b clearly indicating that the generated gas is hydrogen. Additionally, the stability of these photoelectrodes was tested by chronoamperometric measurements. The electrodes showed to be stable (no decrease of photocurrent during more than 1 hour, and the loss of performance detected was due to the depletion of the sacrificial agent in the solution (see Supporting Information, Figure SI5).

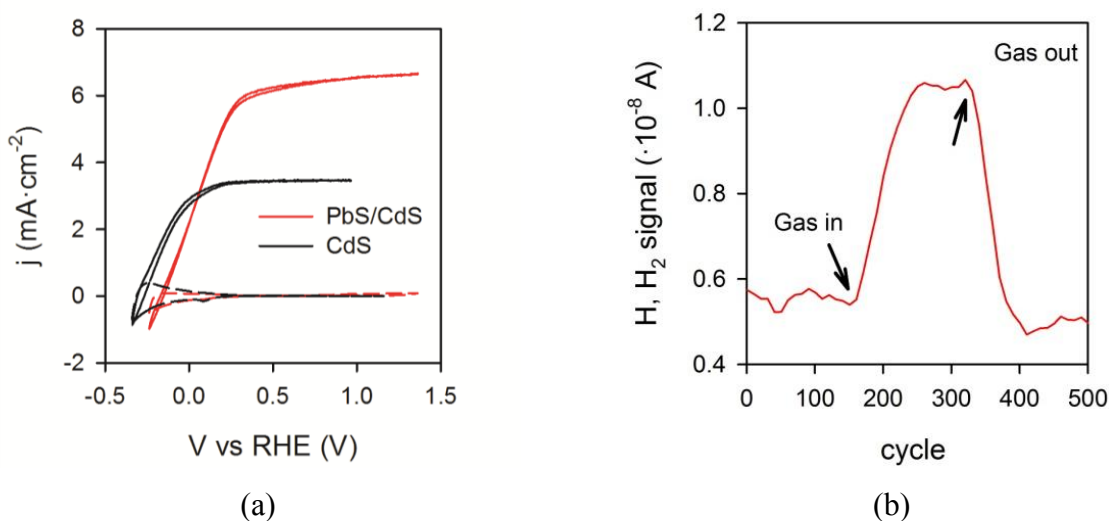


**Figure 1.-** (a) j-V curves for the TiO<sub>2</sub>/CdS/PbS heterostructure in the dark and under illumination (100 mW·cm<sup>-2</sup>) in three electrode configuration, TiO<sub>2</sub>/CdS is also included as a reference (b) Gas chromatography Mass Spectroscopy plot of the evolved gas for TiO<sub>2</sub>/CdS/PbS heterostructure. The signal of H<sub>2</sub> is clearly increased after gas is passed through the system.

The results obtained from the photoelectrochemical characterization showed in Figure 1a suggest that TiO<sub>2</sub>, PbS and CdS form a cascaded structure, and photogenerated electrons at both CdS and PbS can be collected at the contact. Figure 2 shows a proposed energy diagram in which the different electronic processes and relevant electrochemical reactions are scheduled. Further quantification of the position of the energy levels of the conduction and valence band edges for

QDs is out of the scope of the present study. Extensive discussion of the reaction mechanisms has been reported elsewhere.<sup>14, 15, 17, 22, 23</sup> The presence of Na<sub>2</sub>S and Na<sub>2</sub>SO<sub>3</sub> hole scavengers in the electrolyte provides a fast shuttle for the photogenerated holes (reaction 1) avoiding photocorrosion, while electrons are driven through TiO<sub>2</sub> toward the contact, and then to the catalytic cathode, where hydrogen generation takes place (reaction 3).

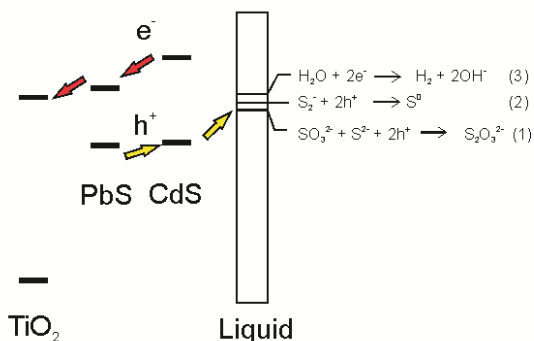


**Figure 2.** Energy diagram illustrating the oxidation at PbS/CdS QDs-sensitized TiO<sub>2</sub> particulate anodes. Energy levels were adapted from<sup>24, 25</sup>. The arrows indicate the traffic of electrons and holes.

In order to gain further insight into the charge transfer mechanisms of TiO<sub>2</sub>/PbS/CdS heterostructures, chopped light j-V curves were carried out. Figure 3a shows the superimposed chopped and constant light j-V curves. The presence of anodic and cathodic transients in the chopped light curve provides direct evidence of the participation of surface states in the hole transfer process. Indeed, the presence of these transients has been attributed to the charging (trapping of holes) of surface states, or oxidizing surface species.<sup>26-28</sup> We have previously showed that when CdS/CdSe quantum dots are used as light absorbers, the hole collection efficiency is unity.<sup>29</sup> On the other hand, we have also showed that the CdS coating on TiO<sub>2</sub>/PbS does not only protect PbS from photocorrosion in polysulfide electrolytes, but also hinders recombination of photoinjected electrons.<sup>18</sup> Conversely, PbS has showed to enhance charge recombination in QDSC as the PbS QD loading increases, possibly due to the participation of surface states in the charge transfer mechanism.<sup>18</sup>

In order to assess the contribution of infrared photons to the higher photocurrent measured for TiO<sub>2</sub>/PbS/CdS (and hence to the H<sub>2</sub> generation), the incident-photon-to-current-efficiency

(IPCE) action spectrum was obtained in a three electrode configuration, at 0.95 V vs RHE. The results for TiO<sub>2</sub>/CdS are also showed as a reference (see Figure 3b). The IPCE action spectrum for TiO<sub>2</sub>/CdS extends up to 550 nm, while when PbS is included in the heterostructure, the wavelength range expands beyond 800 nm, confirming the contribution of infra-red photons to the photocurrent. Indeed, the IPCE action spectrum practically mimics the optical density, and the APCE (absorbed photon to current efficiency) values are practically identical to IPCE as showed in Supporting Information, Figure SI6 for TiO<sub>2</sub>/PbS/CdS. Integration of the IPCE spectrum with wavelength led to a total photocurrent of 5.7 mA·cm<sup>-2</sup> and 4.1 mA·cm<sup>-2</sup> for TiO<sub>2</sub>/PbS/CdS and TiO<sub>2</sub>/CdS, respectively (Figure 3b) in excellent agreement with the maximum photocurrent showed in Figure 1 (6 mA·cm<sup>-2</sup> and 3.5 mA·cm<sup>-2</sup>, respectively).

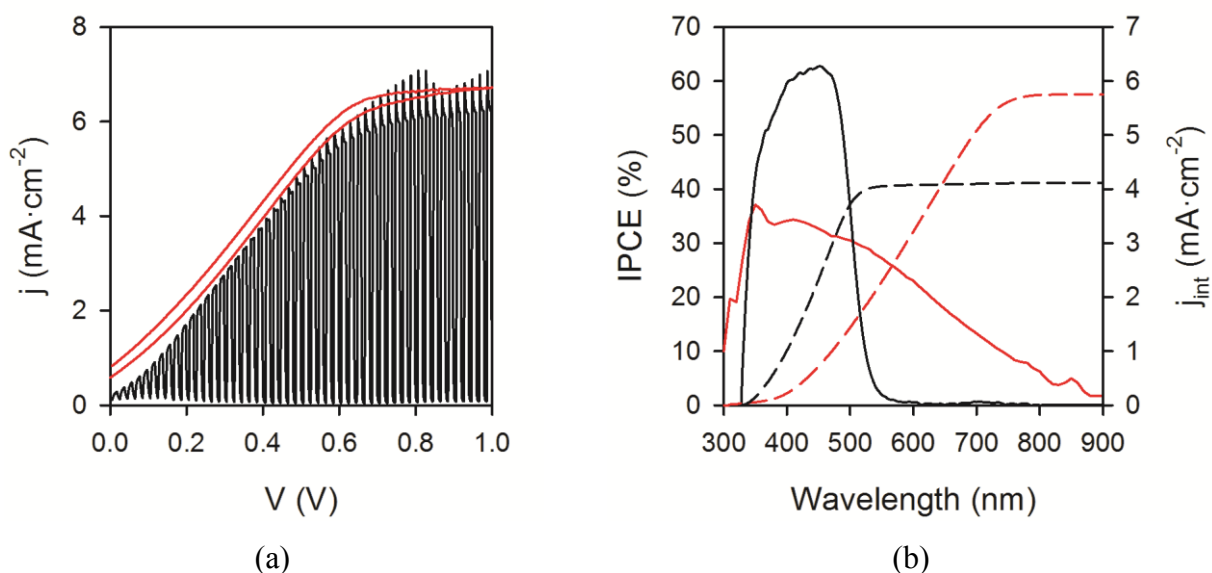


**Figure 3.-** (a) Chopped light (black) and constant (red) illumination  $j$ - $V$  curves in two electrode configuration of the TiO<sub>2</sub>/PbS/CdS heterostructured photoanode. (b) IPCE (solid lines) and integrated current (dashed lines) for a TiO<sub>2</sub>/PbS/CdS (red) and a reference TiO<sub>2</sub>/CdS (black) photoelectrode at 0.95 V vs RHE.

Further photoelectrochemical characterization of the heterostructured TiO<sub>2</sub>/PbS/CdS photoanodes was carried out by impedance spectroscopy measurements in the dark and under illumination. A sound physical model was already developed for similar heterostructured materials,<sup>18, 29-31</sup> which is scheduled as supporting information, Figure SI7. Consequently, this

model was directly applied to extract the chemical capacitance of  $\text{TiO}_2$ ,  $C_\mu$ , the recombination resistance,  $R_{\text{rec}}$  and the transport resistance,  $R_{\text{tr}}$  of the  $\text{TiO}_2/\text{PbS}/\text{CdS}$  architectures.  $C_\mu$  monitors the density of states (DOS) at the Fermi level, and provides the distribution of trap states below the conduction band of  $\text{TiO}_2$ ,  $R_{\text{tr}}$  is directly proportional to the reciprocal conductivity of  $\text{TiO}_2$  ( $\rho_{\text{TiO}_2}$ ) and  $R_{\text{rec}}$  is inversely proportional to the recombination rate of electrons at the  $\text{TiO}_2/\text{solution}$  interface.<sup>19, 32, 33</sup> The exponential behavior of the transport resistance with voltage in the QD sensitized films follows identical exponential trend as compared to bare and dye sensitized  $\text{TiO}_2$ , suggesting that electron transport occurs mainly through the  $\text{TiO}_2$  nanoparticles rather than through QDs.<sup>20</sup> Furthermore, the transport resistance ( $R_{\text{tr}}$ ) for  $\text{TiO}_2$  is very similar in the dark and under illumination (Figure 4a). This is an expected result, since the conductivity of the  $\text{TiO}_2$  nanoparticles is determined by the electron density in the conduction band which, is controlled by the applied potential and not by illumination. The chemical capacitance (Figure 4b) shows the characteristic exponential dependence with potential, reflecting the trap state distribution below the conduction band of  $\text{TiO}_2$ . This agrees well with the assumption that charge is accumulated and transported mainly through the  $\text{TiO}_2$ . The behavior of  $C_\mu$  is very similar in the dark and under illumination conditions again, since it is determined by the position of the Fermi level which is governed by the applied bias. The small difference found at the intermediate states between dark and illumination conditions may be due to a capacitive contribution from the accumulation of charges in the QDs.

Finally, the recombination resistance,  $R_{\text{rec}}$  is governing the photoelectrochemical behavior of the heterostructure, since the total resistance obtained by derivation of the  $j$ - $V$  curve, practically mimics the  $R_{\text{rec}}$  values obtained by impedance spectroscopy both in the dark (Figure 4c) and under illumination (Figure 4d). Therefore, impedance spectroscopy appears as a very attractive experimental technique to monitor the main processes controlling the performance of these materials.



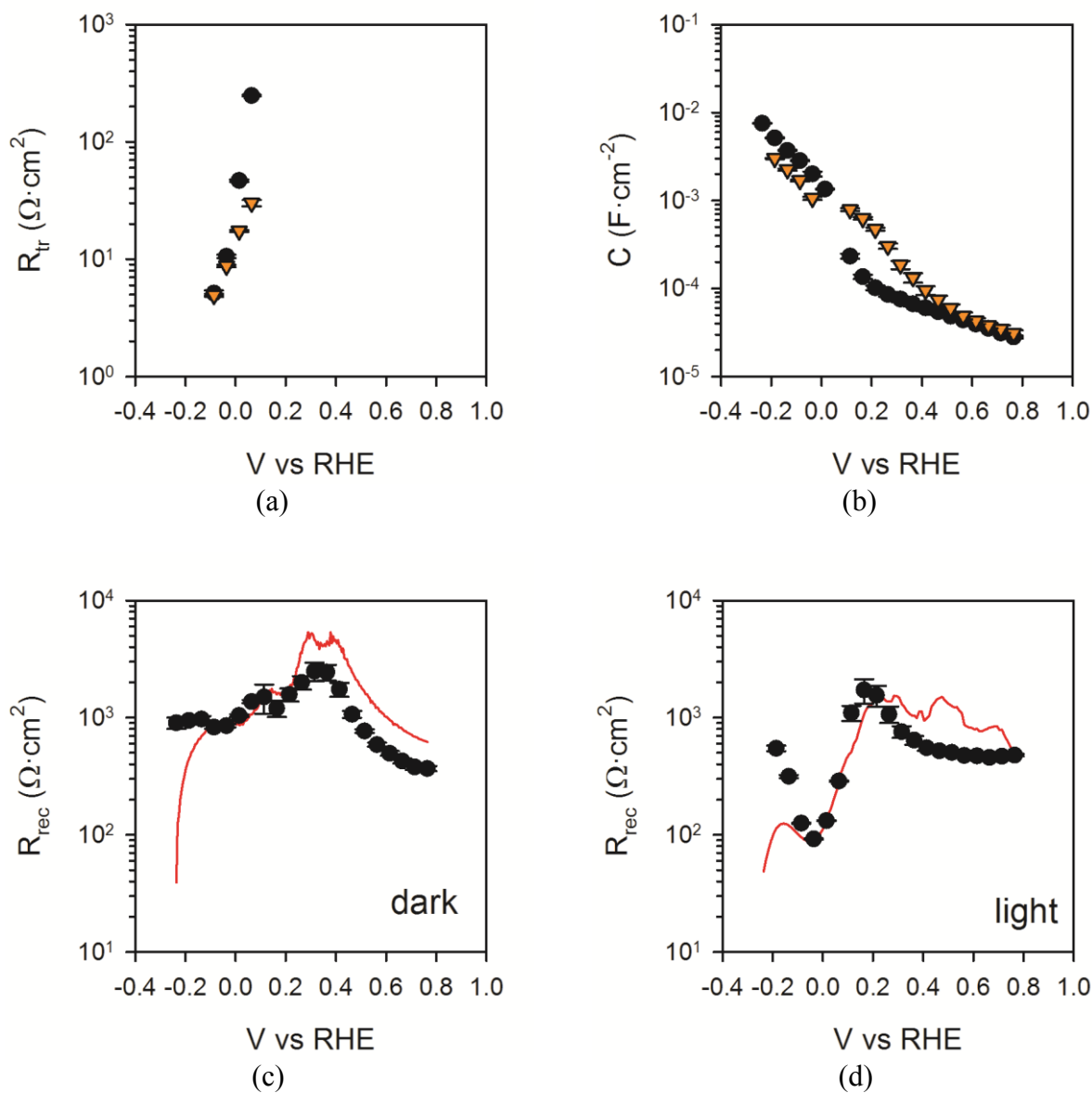
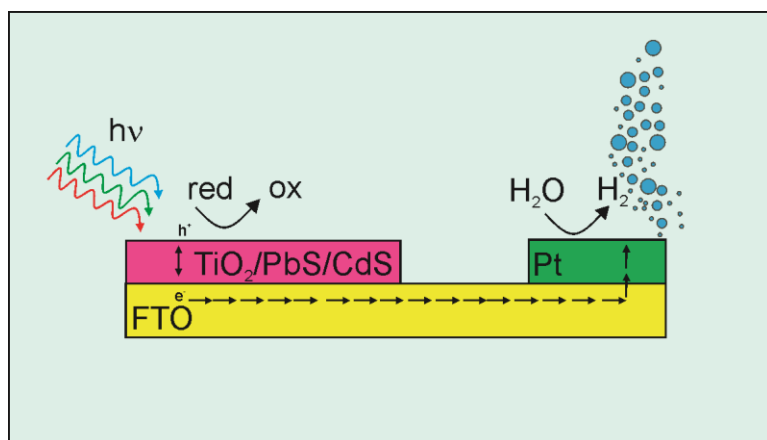


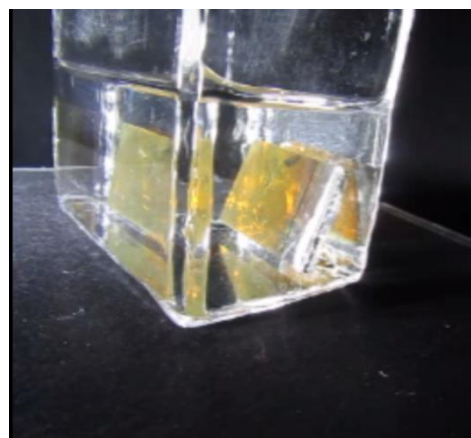
**Figure 4.-** Parameters extracted after fitting the impedance spectroscopy spectra of the heterostructured TiO<sub>2</sub>/PbS/CdS photoanodes, using the model previously developed.<sup>29-31</sup> (a) Transport resistance,  $R_{tr}$ , (b) Chemical capacitance,  $C_{\mu}$ , (c) recombination resistance,  $R_{rec}$  as a function of potential both in the dark and (d) under illumination. The red lines in (c) and (d) represent the total resistance extracted from derivation of the  $j$ - $V$  curve,  $R = \left(\frac{dj}{dV}\right)^{-1}$ . Error bars assigned to the experimental points have been obtained from the fitting error.

From all the above results, TiO<sub>2</sub>/PbS/CdS photoanodes show promising capabilities to drive solar H<sub>2</sub> generation. In order to test the suitability of this configuration for unassisted H<sub>2</sub>

generation, we assembled a wireless device, resembling an artificial leaf<sup>34, 35</sup> as scheduled in Figure 5(a). The device is immersed into the aqueous solution, and upon illumination, electro-hole pairs are photogenerated in the light absorber (PbS/CdS QDs). The holes are quickly injected in the solution driving the sacrificial oxidation of  $\text{SO}_3^{2-}$ . On the other hand, photogenerated electrons are transported through the  $\text{TiO}_2$  mesoporous structure toward the FTO substrate and then to the catalytic cathode, which is composed by a calcined chloroplatinic solution, where hydrogen can evolve. Hydrogen evolution is observed as showed in Figure 5(b) and Supporting Information, audiovisual material. The hydrogen generation rate was 0.18 ml during 1 hour of measurement, which equals  $(4.30 \pm 0.25) \text{ ml} \cdot \text{cm}^{-2} \cdot \text{day}^{-1}$ . It is important to highlight that at this stage, this device cannot be termed “artificial leaf” since the use of a sacrificial agent is needed for operation. However, we believe that this “quasi-artificial leaf” constitutes a promising structure for future developments and different optimization strategies are under investigation in our lab to improve the device efficiency, stability and autonomy. Particularly, morphological optimization of the  $\text{TiO}_2$  structure is an important issue to be addressed, since it has been proven that structures with lower surface area lead to better performance of quantum dot sensitized solar cells based on these structures.<sup>36</sup> Doping has also demonstrated to enhance  $\text{TiO}_2$  conductivity and minimize transport losses.<sup>14</sup> Additionally, the presence of PbS enhances charge recombination, (the lower IPCE values in the range 350-550 nm when PbS is included in the structure is a good evidence) and efficient passivation strategies need to be developed as previously done with colloidal PbS QDs.<sup>37</sup>



(a)



(b)

**Figure 5.-** (a) Scheme of a “quasi-artificial leaf” based on a heterostructured TiO<sub>2</sub>/PbS/CdS photoanode and Pt as cathode. (b) The TiO<sub>2</sub>/PbS/CdS “quasi-artificial leaf” in a quartz cuvette filled with an aqueous 0.25 M Na<sub>2</sub>S and 0.35 M Na<sub>2</sub>SO<sub>3</sub> electrolyte evolving H<sub>2</sub> under illumination. A video of the PbS artificial leaf working autonomously is available in Supporting Information.

### Summary and conclusions

In summary, TiO<sub>2</sub>/PbS/CdS heterostructures have demonstrated to be candidate architectures for hydrogen generation ( $6 \text{ mA} \cdot \text{cm}^{-2}$  or  $60 \text{ ml} \cdot \text{cm}^{-2} \cdot \text{day}^{-1}$ ). Photocurrent and IPCE measurements have confirmed the contribution of infrared photons to the photocurrent leading to H<sub>2</sub> generation. Solar IR radiation provides a huge pool of photons, and consequently of usable energy, which can be stored using the appropriate materials, as PbS, that in spite of its large potentiality has received less attention than visible light harvesters. The integrated current perfectly agrees with that obtained by cyclic voltammetry, and an excellent spectral match between photocurrent and light harvesting has been obtained. Additionally, impedance spectroscopy appears as a simple and reliable characterization tool to inspect the limiting factors affecting the photoelectrochemical performance of the device. We showed that the recombination resistance ( $R_{\text{rec}}$ ) controls the dynamics of the system and further improvement of these heterostructures should be focused on strategies leading to the optimization of the TiO<sub>2</sub> architecture and minimization of charge recombination. Furthermore, IS analysis suggests that transport and accumulation of charge in the film mainly takes place within the TiO<sub>2</sub> nanoparticles. Based on this composite material, we have presented a “quasi-artificial leaf”, which has proven to produce hydrogen under simulated solar illumination at  $(4.30 \pm 0.25) \text{ ml} \cdot \text{cm}^{-2} \cdot \text{day}^{-1}$ . Further developments at our lab focus on the elimination of the sacrificial agent in order to increase the robustness of the developed photoelectrodes. We believe that the present study constitutes an important milestone for the development of systems able to autonomously generate hydrogen combining the advances of nanotechnology and novel optoelectronic concepts.

### Experimental method

Commercial titania paste (Solarnix DSL 18NR, Switzerland, 20 nm particle size) was coated on FTO (SnO<sub>2</sub>:F, TEC 15) substrate by doctor blade technique and then dried at 80° C. Prior to TiO<sub>2</sub> nanoparticle deposition, the FTO substrates were covered by a compact layer of TiO<sub>2</sub>

deposited by spray pyrolysis of titanium(IV)bis(acetoacetonato) di(isopropanoxylate). These electrodes were subsequently sintered at 450 °C for 30 min. The thickness of the electrodes was ~12 μm, as measured by contact profilometry. The titania electrodes were sensitized with PbS QDs grown by Successive Ionic Layer Adsorption and Reaction (SILAR).<sup>18</sup> For this purpose a Pb(CH<sub>3</sub>COO)<sub>2</sub> 0.02 M ethanolic solution was used as Pb<sup>2+</sup> source and another one containing Na<sub>2</sub>S 9 H<sub>2</sub>O 0.02M in methanol/water (50/50 V/V) as sulfide precursor. A single SILAR cycle consisted of 30 seconds dip-coating of the electrode into the lead precursor and then into the sulfide solution, also during 30 seconds. After each precursor bath, the photoanode was thoroughly rinsed by immersion in ethanol and dried. One cycle was sufficient for an adequate PbS sensitization.

For the hybrid PbS/CdS samples, the CdS deposition was carried out immediately after PbS deposition. For CdS SILAR deposition a Cd(CH<sub>3</sub>COO)<sub>2</sub> 0.05 M was used as metal precursor and Na<sub>2</sub>S 9 H<sub>2</sub>O 0.02M in methanol/water (50/50 V/V) as sulfide precursor. SILAR procedure was repeated five times. CdS coating demonstrated to provide an effective protection of PbS from sulfide based electrolytes and an significant enhancement of the stability. After sensitization, all the samples have been coated with ZnS, by dipping alternately into 0.1M Zn(CH<sub>3</sub>COO)<sub>2</sub> (in water) and 0.1M Na<sub>2</sub>S solutions for 1 min/dip, rinsing with Milli-Q ultrapure water between dips (2 cycles).<sup>38</sup> Reference “only CdS” samples have been produced, following the same steps described above, except the deposition of PbS.

Structural inspection of the samples was carried out using a JEOL JEM-3100F field emission scanning electron microscope (SEM) and a JEOL JSM 7600F field emission transmission electron microscope (TEM). The crystallographic structure of the samples was tested by X-ray diffraction (XRD). The optical density of the photoelectrodes were recorded between 300 and 800 nm by a Cary 500 UV-VIS Varian spectrophotometer.

The transmittance spectra of the photoelectrodes were recorded between 300 and 800 nm by a Cary 500 UV-VIS Varian spectrophotometer. Steady state and chopped light current density voltage (j-V), Electrochemical Impedance Spectroscopy (EIS) and V<sub>oc</sub> decay measurements were carried out using a FRA equipped PGSTAT-30 from Autolab. A three-electrode configuration

was used, where the TiO<sub>2</sub>/PbS/CdS photo-electrode was connected to the working electrode, a Pt wire was connected to the counterelectrode and a saturated Ag/AgCl electrode was used as reference. An aqueous solution containing 0.25 M Na<sub>2</sub>S and 0.35 M Na<sub>2</sub>SO<sub>3</sub> as sacrificial hole scavenger was used as the electrolyte to prevent photocorrosion of the QDs. Nitrogen was bubbled during 30min before testing to avoid the presence of oxygen (electron acceptor) in the solution. The pH of the solution was 13 and all the electrochemical measurements were referred to the reversible hydrogen electrode (RHE) by the equation  $V_{RHE} = V_{Ag/AgCl} + 0.197 + pH(0.059)$ . The electrodes were illuminated using a 450 W Xe lamp (Oriel), where the light intensity was adjusted with a thermopile to 100 mW/cm<sup>2</sup>, with illumination through the substrate. EIS measurements were carried out applying 20 mV AC signal and scanning in a frequency range between 400 kHz and 0.1 Hz, at different applied biases. The IPCE measurements were carried out by employing a 300 W Xe lamp coupled with a computer-controlled monochromator; the photoelectrode was polarized at the desired voltage with a Gamry potentiostat and the photocurrent was measured using an optical power meter 70310 from Oriel Instruments. Labeling experiments of the evolved gases were carried out using gas chromatography mass spectroscopy GC/MS. A quadrupole Pfeiffer Vacuum model Thermostar GSD301T with a mass interval ranging down to 300 uma was used. The evolved gas was collected in an inverted burette and extracted with a gas-tight syringe provided with an exit valve.

### **Acknowledgements**

We acknowledge support by projects from Ministerio de Economía y Competitividad (MINECO) of Spain (Consolider HOPE CSD2007-00007, MAT2010-19827), Generalitat Valenciana (PROMETEO/2009/058 and project ISIC/2012/008 “Institute of Nanotechnologies for Clean Energies”) and Fundació Bancaixa (P1.1B2011-50). S. Gimenez acknowledges support by MINECO of Spain under the Ramon y Cajal programme. The SCIC of the University Jaume I de Castello is also acknowledged for the gas analysis measurements. C. Sima acknowledges the POSDRU/89/1.5/S/58852 Project, “Postdoctoral programme for training scientific researchers” cofinanced by the European Social Fund within the Sectorial Operational Program Human Resources Development 2007-2013.

**Supporting Information Available:** TiO<sub>2</sub>/CdS and TiO<sub>2</sub>/PbS/CdS light absorption, SEM image, XRD of TiO<sub>2</sub>/PbS electrodes, TEM micrograph, stability, IPCE vs. light absorption and APCE, impedance model and a video of the PbS artificial leaf working autonomously. This material is available free of charge *via* the Internet at <http://pubs.acs.org>.

## References

1. Crabtree, G. W.; Lewis, S. N., Solar Energy Conversion. *Physics Today* 2007, 60, 37-42.
2. Walter, M. G.; Warren, E. L.; McKone, J. R.; Boettcher, S. W.; Mi, Q. X.; Santori, E. A.; Lewis, N. S., Solar Water Splitting Cells. *Chemical Reviews* 2010, 110, 6446-6473.
3. Cook, T. R.; Dogutan, D. K.; Reece, S. Y.; Surendranath, Y.; Teets, T. S.; Nocera, D. G., Solar Energy Supply and Storage for the Legacy and Non legacy Worlds. *Chemical Reviews* 2010, 110, 6474-6502.
4. van de Krol, R.; Liang, Y. Q.; Schoonman, J., Solar hydrogen production with nanostructured metal oxides. *Journal of Materials Chemistry* 2008, 18, 2311-2320.
5. Fujishima, A.; Honda, K., *Nature* 1972, 238, 37-38.
6. Tilley, S. D.; Cornuz, M.; Sivula, K.; Gratzel, M., Light-Induced Water Splitting with Hematite: Improved Nanostructure and Iridium Oxide Catalysis. *Angewandte Chemie-International Edition* 2010, 49, 6405-6408.
7. Kelzenberg, M. D.; Boettcher, S. W.; Petykiewicz, J. A.; Turner-Evans, D. B.; Putnam, M. C.; Warren, E. L.; Spurgeon, J. M.; Briggs, R. M.; Lewis, N. S.; Atwater, H. A., Enhanced absorption and carrier collection in Si wire arrays for photovoltaic applications. *Nature Materials* 2010, 9, 239-244.
8. Lin, Y. J.; Yuan, G. B.; Liu, R.; Zhou, S.; Sheehan, S. W.; Wang, D. W., Semiconductor nanostructure-based photoelectrochemical water splitting: A brief review. *Chemical Physics Letters* 2011, 507, 209-215.
9. Lin, Y. J.; Yuan, G. B.; Sheehan, S.; Zhou, S.; Wang, D. W., Hematite-based solar water splitting: challenges and opportunities. *Energy & Environmental Science* 2011, 4, 4862-4869.
10. Holmes, M. A.; Townsend, T. K.; Osterloh, F. E., Quantum confinement controlled photocatalytic water splitting by suspended CdSe nanocrystals. *Chemical Communications* 2012, 48, 371-373.
11. Yang, S. Y.; Prendergast, D.; Neaton, J. B., Tuning Semiconductor Band Edge Energies for Solar Photocatalysis via Surface Ligand Passivation. *Nano Letters* 2012, 12, 383-388.
12. Thimsen, E.; Le Formal, F.; Gratzel, M.; Warren, S. C., Influence of Plasmonic Au Nanoparticles on the Photoactivity of Fe(2)O(3) Electrodes for Water Splitting. *Nano Letters* 2011, 11, 35-43.
13. Thomann, I.; Pinaud, B. A.; Chen, Z. B.; Clemens, B. M.; Jaramillo, T. F.; Brongersma, M. L., Plasmon Enhanced Solar-to-Fuel Energy Conversion. *Nano Letters* 2011, 11, 3440-3446.
14. Hensel, J.; Wang, G. M.; Li, Y.; Zhang, J. Z., Synergistic Effect of CdSe Quantum Dot Sensitization and Nitrogen Doping of TiO(2) Nanostructures for Photoelectrochemical Solar Hydrogen Generation. *Nano Letters* 2010, 10, 478-483.
15. Chen, H. M.; Chen, C. K.; Chang, Y. C.; Tsai, C. W.; Liu, R. S.; Hu, S. F.; Chang, W. S.; Chen, K. H., Quantum Dot Monolayer Sensitized ZnO Nanowire-Array Photoelectrodes: True Efficiency for Water Splitting. *Angewandte Chemie-International Edition* 2010, 49, 5966-5969.
16. Kim, H.; Seol, M.; Lee, J.; Yong, K., Highly Efficient Photoelectrochemical Hydrogen Generation Using Hierarchical ZnO/WOx Nanowires Cosensitized with CdSe/CdS. *Journal of Physical Chemistry C* 2011, 115, 25429-25436.

17. Jin-nouchi, Y.; Hattori, T.; Sumida, Y.; Fujishima, M.; Tada, H., PbS Quantum Dot-Sensitized Photoelectrochemical Cell for Hydrogen Production from Water under Illumination of Simulated Sunlight. *Chemphyschem* 2010, 11, 3592-3595.
18. Braga, A.; Gimenez, S.; Concina, I.; Vomiero, A.; Mora-Sero, I., Panchromatic Sensitized Solar Cells Based on Metal Sulfide Quantum Dots Grown Directly on Nanostructured TiO<sub>2</sub> Electrodes. *Journal of Physical Chemistry Letters* 2011, 2, 454-460.
19. Bisquert, J., Chemical capacitance of nanostructured semiconductors: its origin and significance for nanocomposite solar cells. *Physical Chemistry Chemical Physics* 2003, 5, 5360-5364.
20. Fabregat-Santiago, F.; Randriamahazaka, H.; Zaban, A.; Garcia-Canadas, J.; Garcia-Belmonte, G.; Bisquert, J., Chemical capacitance of nanoporous-nanocrystalline TiO<sub>2</sub> in a room temperature ionic liquid. *Physical Chemistry Chemical Physics* 2006, 8, 1827-1833.
21. Guijarro, N.; Lana-Villarreal, T.; Mora-Sero, I.; Bisquert, J.; Gomez, R., CdSe Quantum Dot-Sensitized TiO<sub>2</sub> Electrodes: Effect of Quantum Dot Coverage and Mode of Attachment. *Journal of Physical Chemistry C* 2009, 113, 4208-4214.
22. Chouhan, N.; Yeh, C. L.; Hu, S. F.; Huang, J. H.; Tsai, C. W.; Liu, R. S.; Chang, W. S.; Chen, K. H., Array of CdSe QD-Sensitized ZnO Nanorods Serves as Photoanode for Water Splitting. *Journal of the Electrochemical Society* 2010, 157, B1430-B1433.
23. Smotkin, E. S.; Cerveramarch, S.; Bard, A. J.; Campion, A.; Fox, M. A.; Mallouk, T.; Webber, S. E.; White, J. M., BIPOLAR CDSE/COS SEMICONDUCTOR PHOTOELECTRODE ARRAYS FOR UNASSISTED PHOTOLYTIC WATER SPLITTING. *Journal of Physical Chemistry* 1987, 91, 6-8.
24. Fabregat-Santiago, F.; Garcia-Belmonte, G.; Mora-Sero, I.; Bisquert, J., Characterization of nanostructured hybrid and organic solar cells by impedance spectroscopy. *Physical Chemistry Chemical Physics* 2011, 13, 9083-9118.
25. Haynes, W. M., *Handbook of Chemistry and Physics 83th edition*. CRC Press: 2002.
26. Salvador, P., KINETIC APPROACH TO THE PHOTOCURRENT TRANSIENTS IN WATER PHOTOELECTROLYSIS AT N-TIO<sub>2</sub> ELECTRODES .1. ANALYSIS OF THE RATIO OF THE INSTANTANEOUS TO STEADY-STATE PHOTOCURRENT. *Journal of Physical Chemistry* 1985, 89, 3863-3869.
27. Klahr, B. M.; Gimenez, S.; Fabregat-Santiago, F.; Bisquert, J.; Hamann, T. W., Electrochemical and Photoelectrochemical Investigation of Water Oxidation with Hematite Electrodes. *Energy Environ. Sci.* 2012, 5, 7626-7636.
28. Le Formal, F.; Gratzel, M.; Sivula, K., Controlling Photoactivity in Ultrathin Hematite Films for Solar Water-Splitting. *Advanced Functional Materials* 2010, 20, 1099-1107.
29. Rodenas, P.; Song, T.; Sudhagar, P.; Marzari, G.; Han, H.; Badía-Bou, L.; Gimenez, S.; Fabregat-Santiago, F.; Mora-Sero, I.; Bisquert, J.; Paik, U.; Kang, Y. S., Quantum dot based heterostructures for unassisted photoelectrochemical hydrogen generation. *Advanced Energy Materials* 2012, In press. DOI: 10.1002/aenm.201200255.
30. Gonzalez-Pedro, V.; Xu, X. Q.; Mora-Sero, I.; Bisquert, J., Modeling High-Efficiency Quantum Dot Sensitized Solar Cells. *Acs Nano* 2010, 4, 5783-5790.
31. Mora-Sero, I.; Gimenez, S.; Fabregat-Santiago, F.; Gomez, R.; Shen, Q.; Toyoda, T.; Bisquert, J., Recombination in Quantum Dot Sensitized Solar Cells. *Accounts of Chemical Research* 2009, 42, 1848-1857.
32. Bisquert, J., Theory of the impedance of electron diffusion and recombination in a thin layer. *Journal of Physical Chemistry B* 2002, 106, 325-333.
33. Bisquert, J.; Cahen, D.; Hodes, G.; Ruhle, S.; Zaban, A., Physical chemical principles of photovoltaic conversion with nanoparticulate, mesoporous dye-sensitized solar cells. *Journal of Physical Chemistry B* 2004, 108, 8106-8118.
34. Nocera, D. G., The Artificial Leaf. *Accounts of Chemical Research* 2012, 45, 767-776.

35. Reece, S. Y.; Hamel, J. A.; Sung, K.; Jarvi, T. D.; Esswein, A. J.; Pijpers, J. J. H.; Nocera, D. G., Wireless Solar Water Splitting Using Silicon-Based Semiconductors and Earth-Abundant Catalysts. *Science* 2011, 334, 645-648.
36. Samadpour, M.; Gimenez, S.; Iraj Zad, A.; Taghavinia, N.; Calvo, M.; Miguez, H.; Mora-Sero, I., Effect of the architecture of TiO<sub>2</sub> and QDs deposition strategy on the photovoltaic performance of Quantum Dot Sensitized Solar Cells. *Electrochimica Acta* 2012, 75, 139-147.
37. Tang, J.; Kemp, K. W.; Hoogland, S.; Jeong, K. S.; Liu, H.; Levina, L.; Furukawa, M.; Wang, X. H.; Debnath, R.; Cha, D. K.; Chou, K. W.; Fischer, A.; Amassian, A.; Asbury, J. B.; Sargent, E. H., Colloidal-quantum-dot photovoltaics using atomic-ligand passivation. *Nature Materials* 10, 765-771.
38. Shen, Q.; Kobayashi, J.; Diguna, L. J.; Toyoda, T., Effect of ZnS coating on the photovoltaic properties of CdSe quantum dot-sensitized solar cells. *Journal of Applied Physics* 2008, 103.



## Figure captions

**Figure 1.-** (a) j-V curves for the TiO<sub>2</sub>/CdS/PbS heterostructure in the dark and under illumination (100 mW·cm<sup>-2</sup>) in three electrode configuration, TiO<sub>2</sub>/CdS is also included as a reference (b) Gas chromatography Mass Spectroscopy plot of the evolved gas for TiO<sub>2</sub>/CdS/PbS heterostructure. The signal of H<sub>2</sub> is clearly increased after gas is passed through the system.

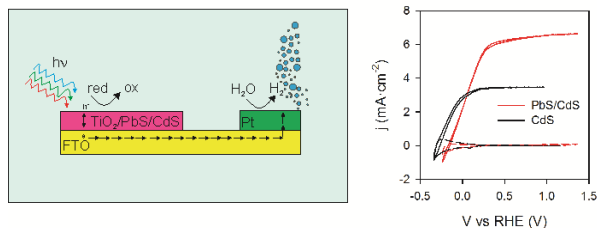
**Figure 2.** Energy diagram illustrating the oxidation at PbS/CdS QDs-sensitized TiO<sub>2</sub> particulate anodes. Energy levels were adapted from<sup>24, 25</sup>. The arrows indicate the traffic of electrons and holes.

**Figure 3.-** (a) Chopped light (black) and constant (red) illumination j-V curves in two electrode configuration of the TiO<sub>2</sub>/PbS/CdS heterostructured photoanode. (b) IPCE (solid lines) and integrated current (dashed lines) for a TiO<sub>2</sub>/PbS/CdS (red) and a reference TiO<sub>2</sub>/CdS (black) photoelectrode at 0.95 V vs RHE.

**Figure 4.-** Parameters extracted after fitting the impedance spectroscopy spectra of the heterostructured TiO<sub>2</sub>/PbS/CdS photoanodes, using the model previously developed.<sup>29-31</sup> (a) Transport resistance, R<sub>tr</sub>, (b) Chemical capacitance (C<sub>μ</sub>), (c) recombination resistance (R<sub>rec</sub>) as a function of potential both in the dark and (d) under illumination. The red lines in (c) and (d) represent the total resistance extracted from derivation of the j-V curve,  $R = \left(\frac{dj}{dV}\right)^{-1}$ . Error bars assigned to the experimental points have been obtained from the fitting error.

**Figure 5.-** (a) Scheme of a “quasi-artificial leaf” based on a heterostructured TiO<sub>2</sub>/PbS/CdS photoanode and Pt as cathode. (b) The TiO<sub>2</sub>/PbS/CdS “quasi-artificial leaf” in a quartz cuvette filled with an aqueous 0.25 M Na<sub>2</sub>S and 0.35 M Na<sub>2</sub>SO<sub>3</sub> electrolyte evolving H<sub>2</sub> under illumination. A video of the PbS artificial leaf working autonomously is available in Supporting Information, audiovisual material.

## Table of Contents (TOC)



Here we present a Quantum Dot based “quasi-artificial leaf”, based on a TiO<sub>2</sub>/PbS/CdS heterostructured nanocomposite electrode. The device has demonstrated to produce 4.30 ml·cm<sup>-2</sup>·day<sup>-1</sup> H<sub>2</sub>, confirmed through labeling experiments. The photoelectrochemical characterization of the material also provided an accurate description of the transport and accumulation of charge carriers in the device.

